Journal of Power Sources 222 (2013) 261–266

Contents lists available at SciVerse ScienceDirect

Journal of Power Sources

journal homepage: www.elsevier.com/locate/jpowsour

Enhanced electrocatalysis of PtRu onto graphene separated by Vulcan carbon spacer

Seunghee Woo [a], Jaeyoung Lee [b], Seung-Keun Park [c], Hasuck Kim [d], Taek Dong Chung [a,**], Yuanzhe Piao [c,e,*]

[a] Department of Chemistry, Seoul National University, Seoul 151-747, Republic of Korea
[b] School of Environmental Science and Engineering, Ertl Center for Electrochemistry and Catalysis, Gwangju Institute of Science and Technology, Gwangju 500-712, Republic of Korea
[c] Department of Nano Science and Technology, Graduate School of Convergence Science and Technology, Seoul National University, Suwon 443-270, Republic of Korea
[d] Department of Energy Systems Engineering, Daegu Gyeongbuk Institute of Science and Technology, Daegu 711-874, Republic of Korea
[e] Advanced Institutes of Convergence Technology, Suwon 443-270, Republic of Korea

HIGHLIGHTS

- Vulcan carbon is added as a nano spacer to enhance the utilization and electrochemical activities.
- The suggested structure provides more triple-phase boundaries available for electrochemical reaction.
- The PtRu/graphene–Vulcan carbon (3:1 w/w) exhibits the highest methanol oxidation current density.
- The prepared catalyst shows better mass transport in the PEMFC.

GRAPHICAL ABSTRACT

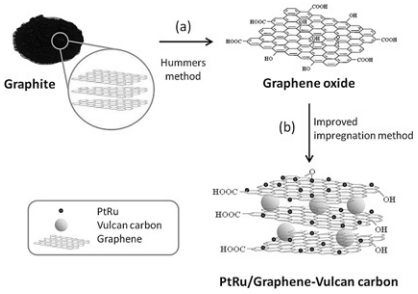

ARTICLE INFO

Article history:
Received 12 May 2012
Received in revised form
18 June 2012
Accepted 31 July 2012
Available online 1 September 2012

Keywords:
Graphene
Vulcan carbon
Platinum
Ruthenium
Methanol oxidation
Polymer electrolyte membrane fuel cell

ABSTRACT

For low temperature polymer fuel cells, carbon supporting material is an important factor that may affect the performance of supported electrocatalysts owing to interactions and surface reactivity. In this research, we design a well-arranged structure of graphene–Vulcan carbon composite to prepare highly dispersed 40 wt.% PtRu electrocatalysts. The Vulcan carbon is added as a nano spacer to enhance electrocatalytic activities of the PtRu catalysts in a methanol oxidation and fuel cell performance resulting in its higher utilization efficiency. The results show that Vulcan carbon is effectively designed to array of graphene sheets, resulting in more triple-phase boundaries available for electrochemical reaction and better mass transport in the catalyst layer.

1. Introduction

Carbon is an ideal material for supporting nano-sized metallic particles in an electrode for low temperature polymer fuel cells [1–3]. No materials other than carbon have the essential properties of electronic conductivity, corrosion resistance, surface properties,

* Corresponding author. Tel.: +82 31 888 9141; fax: +82 31 888 9148.
** Corresponding author. Tel.: +82 2 880 4362; fax: +82 2 887 4354.
E-mail addresses: tdchung@snu.ac.kr (T.D. Chung), parkat9@snu.ac.kr (Y. Piao).

0378-7753/$ – see front matter © 2012 Elsevier B.V. All rights reserved.
http://dx.doi.org/10.1016/j.jpowsour.2012.07.115

and low cost required for the commercialization of fuel cells. Recently, graphene has been studied as a catalyst support due to its excellent conductivity, remarkable mechanical strength and high specific surface area [4–13]. Various techniques including mechanical exfoliation, epitaxial growth and chemical vapor deposition have been developed for producing graphene. Among them, chemically synthesized graphene using either graphite or a graphite derivative as the starting material has been found to be a useful component in various composites, potentially improving and controlling their properties [14,15]. In a previous study, we reported that a PtRu/graphene was used as an electrocatalyts for improving methanol oxidation [10]. The surface area of graphene decreases considerably when separated sheets aggregate together due to van der Waals force and $\pi-\pi$ interaction [16–18], this will influence the utility and activity of the catalysts supported on them. Although the use of metal nanoparticles has been proposed for separating the graphene sheets, there has been some difficulty in creating a triple-phase boundary in a catalyst layer.

In this research, we tried to provide a better approach of reactants into PtRu catalysts *via* the addition of a nano-sized spacer between graphene sheets as illustrated in Fig. 1. The Vulcan carbon, the most widely used carbon supporting material in polymer electrolyte membrane fuel cells, could disrupt the preferred horizontal stacking of the graphene sheets. We investigated the effect of the composite ratio between graphene and Vulcan carbon on the electrochemical oxidation characteristics of methanol. We also studied the effect of the PtRu/graphene–Vulcan carbon catalysts in polymer electrolyte membrane fuel cell. The prepared structure provides more triple-phase boundaries to be available for methanol oxidation reaction and fuel cell performance.

2. Experimental methods

2.1. Preparation of graphene oxide

Graphene oxide was synthesized using the modified Hummers method reported by Kovtyukhova et al [19]. Synthesized graphene oxide was suspended in water (0.05 wt.%) to give a brown dispersion. Exfoliation of the graphene oxide was achieved through ultrasonication for 3 h and then subsequently dialyzed (12–14 kDa cut-off) for 6 h to remove any residual salts and acids. The obtained solution was then subjected to 20 min of centrifugation at 3000 rpm to remove any unexfoliated graphene oxide [20,21]. Finally, the precipitate was dried at 70 °C overnight.

2.2. Synthesis of PtRu/graphene–Vulcan carbon composites

A PtRu alloy catalyst supported on graphene–Vulcan carbon was prepared using an improved impregnation method [22], applying HCHO as a reducing agent and HCl as an acidic sedimentation promoter. H_2PtCl_6 (Aldrich) and $RuCl_3$ (Aldrich) were used as metal precursors. The atomic ratio of platinum to ruthenium was adjusted to 1:1. Graphene oxide and Vulcan carbon (VULCAN XC-72, Cabot Corp.) were used as supports to make 40 wt.% PtRu/graphene–Vulcan carbon catalysts. The graphene oxide and Vulcan carbon ratio varied between 0 and 100 wt.%. The prepared catalysts were heat-treated at 300 °C in 10% H_2 in N_2 atmosphere to reduce the oxidized catalysts. For a comparison, 40 wt.% PtRu/graphene and PtRu/Vulcan carbon catalysts were also prepared in the same manner.

2.3. Characterization

The chemical states of the component elements were analyzed through XPS (AXIS-His spectrometer, KRATOS) using a monochromatic Al Ka X-ray source (1486.6 eV) with a 12 kV voltage and 10 mA current. The binding energies were shifted for charging using C 1s to 284.6 eV. The C 1s signals were collected and analyzed based on the deconvolution of the spectra using XPS peak software. Atomic force microscopy (AFM) images of the layers deposited on SiO_2/Si substrates were obtained using a Digital Instruments XE150 (PSIA) in tapping mode. Typical images were obtained at line scan rates of 1 Hz and 256 × 256 pixel samples were collected. A high-resolution transmission electron microscope (HR-TEM, JEM-3010,

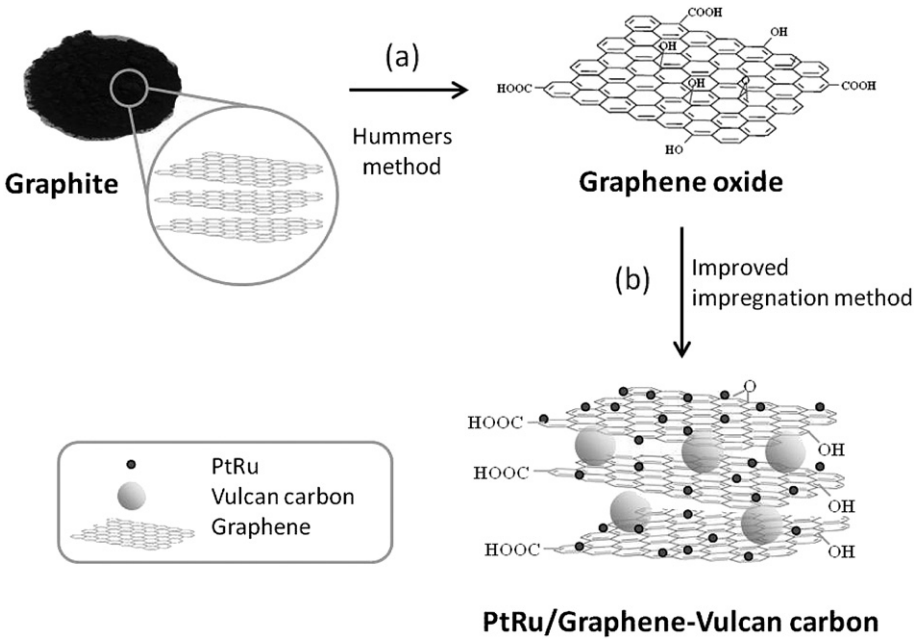

Fig. 1. Schematic illustration of facile synthesis of graphene–Vulcan carbon composite. (a) Chemical oxidation using modified Hummers method and (b) preparation of PtRu/graphene–Vulcan carbon catalyst using an improved impregnation method.

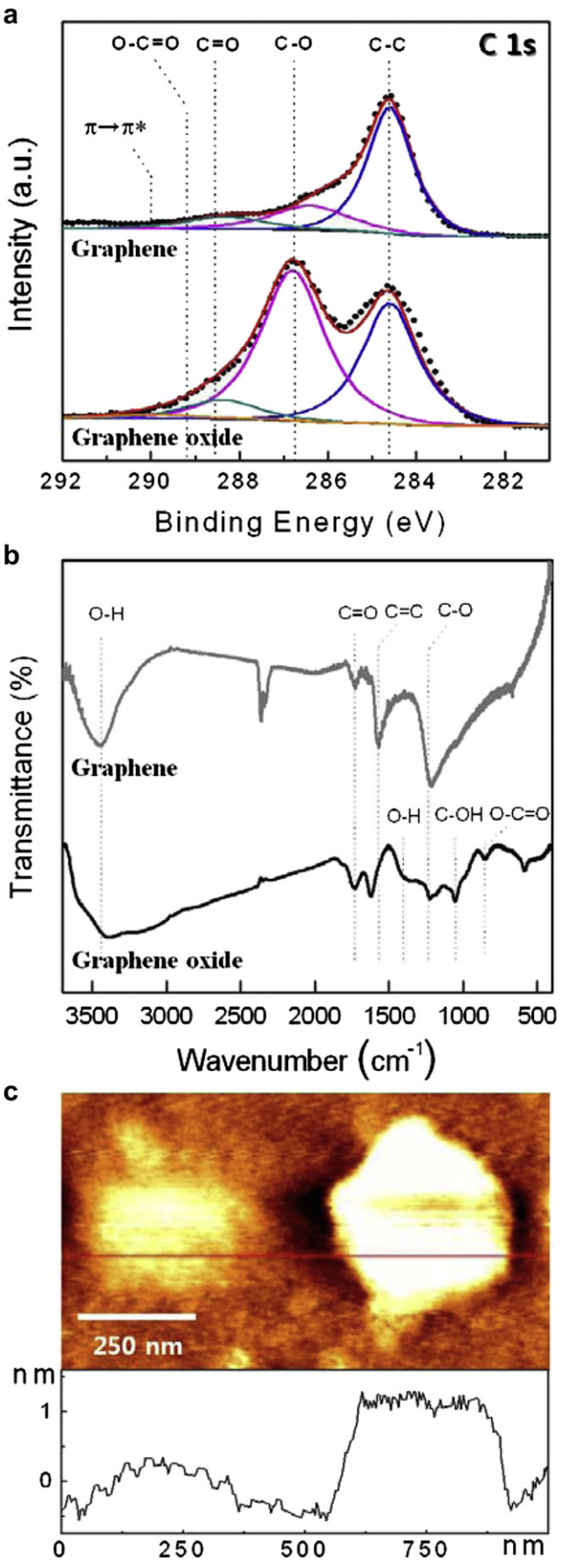

Fig. 2. (a) XPS spectra of graphene oxide and graphene, (b) FT-IR spectra of graphene oxide and graphene, and (c) tapping-mode AFM image of graphene on SiO_2/Si substrate.

JEOL) and field-emission scanning electron microscope (FE-SEM, JSM-6700F, JEOL) were used to check the morphology of the catalysts. The crystallinity of the samples was determined through X-ray diffraction (XRD) performed using a M18XHF-SRA (MAC science Co.) diffractometer equipped with nickel-filtered Cu Ka radiation at a scan rate of 5° min^{-1} (2-theta). The X-ray gun was operated at 50 kV and 200 mA.

2.4. Electrochemical measurements

All electrochemical experiments were performed using an Autolab potentiostat (Metrohm, USA) with a conventional 3-electrode system. The electrochemical cell consists of a glassy carbon electrode (3 mm diameter, Bioanalytical Systems, Inc.) as the working electrode, Ag/AgCl (Bioanalytical Systems, Inc.) as the reference electrode, and platinum wire as the counter electrode. All potentials determined through the electrochemical measurements were converted to the reversible hydrogen electrode (RHE) scale. The scan rate used during the CV measurement was 20 mV s^{-1}. The working electrodes were prepared as follows: a glassy carbon electrode, polished to a mirror finish with a 0.05 mm alumina suspension (Buehler, Lake Bluff, MN, USA) before each experiment, was used as a substrate for the catalysts during the electrochemical measurements. A mixture of the catalyst, 5 wt.% Nafion solution, 2-propanol, and distilled water were ultrasonically homogenized. For the measurements, a thin compact layer of the mixture was cast onto the glassy carbon electrode. A measured volume of this mixture was dropped onto the glassy carbon surface, which enabled the calculation of the catalyst loading. The electrochemical activity of the methanol oxidation reaction was measured using linear sweep voltammetry at a scan rate of 20 mV s^{-1} at 25 °C in a 1 M CH_3OH and 1 M H_2SO_4 solution. The electrochemically active surface area (ESA) of the prepared catalysts was determined using CO-stripping voltammetry in 1 M H_2SO_4 solution. CO adsorption was achieved at 0.1 V versus RHE in a CO saturated solution for 10 minutes and the electrolyte was purged with nitrogen for 10 min to remove CO on the surface. The amount of CO_{ads} was evaluated by integrating the stripping peak of CO_{ads}, which was corrected for the electric double-layer capacitance. The electrochemical surface area of the PtRu metal was obtained using two assumptions: (1) the monolayer of the linearly adsorbed CO was established, and (2) the coulombic charge required for oxidation was 420 mC cm^{-2} [22,23]. Chronoamperometry curves were measured at 0.7 V for 3600 s in 1 M CH_3OH and 1 M H_2SO_4.

2.5. Unit cell test

The polymer electrolyte membrane fuel cell tests of the prepared catalysts were performed with respective anode electrocatalysts under the same operating conditions. To fabricate the membrane electrode assembly (MEA), the catalyst slurry for the electrode was prepared by thoroughly mixing catalysts, Nafion solution (5 wt.%), and an appropriate amount of isopropyl alcohol. The well-mixed slurry was sprayed on a GDL (E-TEK, LT 1200-W) with 0.4 mg_{PtRu} cm^{-2} for the anode. The Pt/C (E-TEK, 40 wt.%) catalyst slurry with 0.4 mg_{pt} cm^{-2} was applied for the cathode. The anode and cathode electrodes were placed on both sides of a Nafion 112 membrane (DuPont). The MEA was hot-pressed at 9800 kPa for 3 min at 130 °C. The cell performance and operating conditions were measured and controlled by a fuel cell test station (Globe

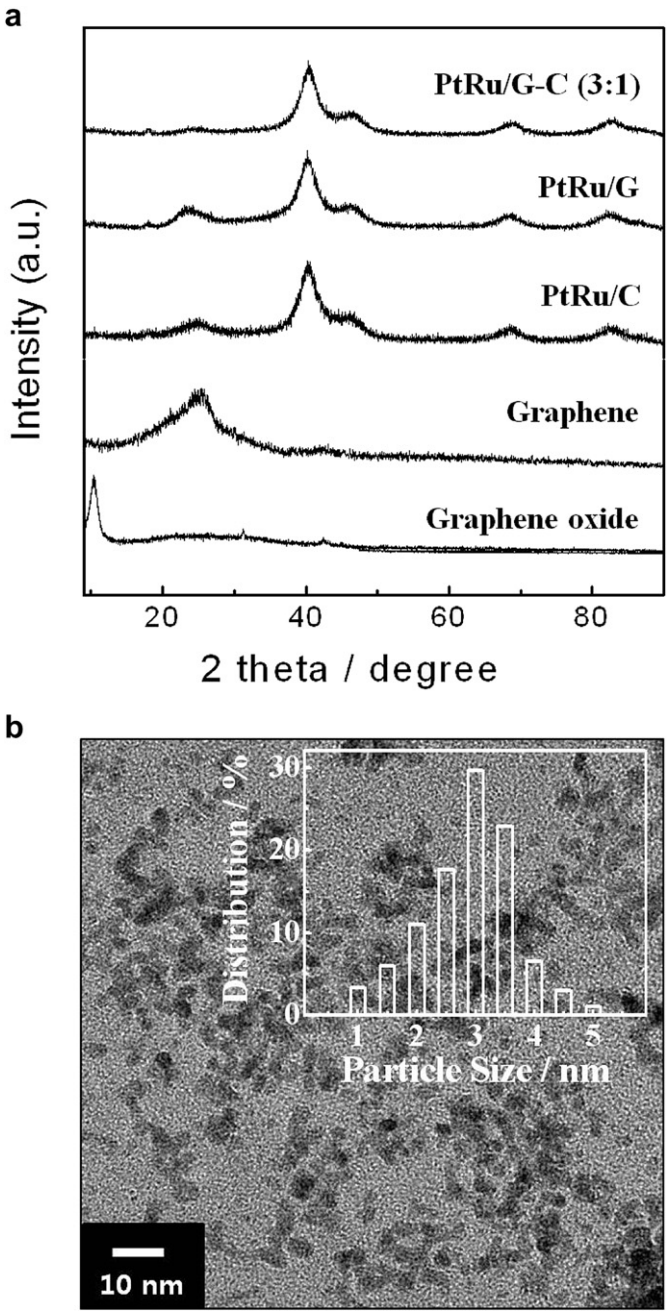

Fig. 3. (a) X-ray diffraction profiles of graphene oxide, graphene, PtRu/Vulcan carbon (PtRu/C), PtRu/graphene (PtRu/G), and PtRu/graphene–Vulcan carbon (PtRu/G–C (3:1)) and (b) HR-TEM image of PtRu metal particles anchored onto graphene–Vulcan carbon. The inset is a graph of particle size distribution.

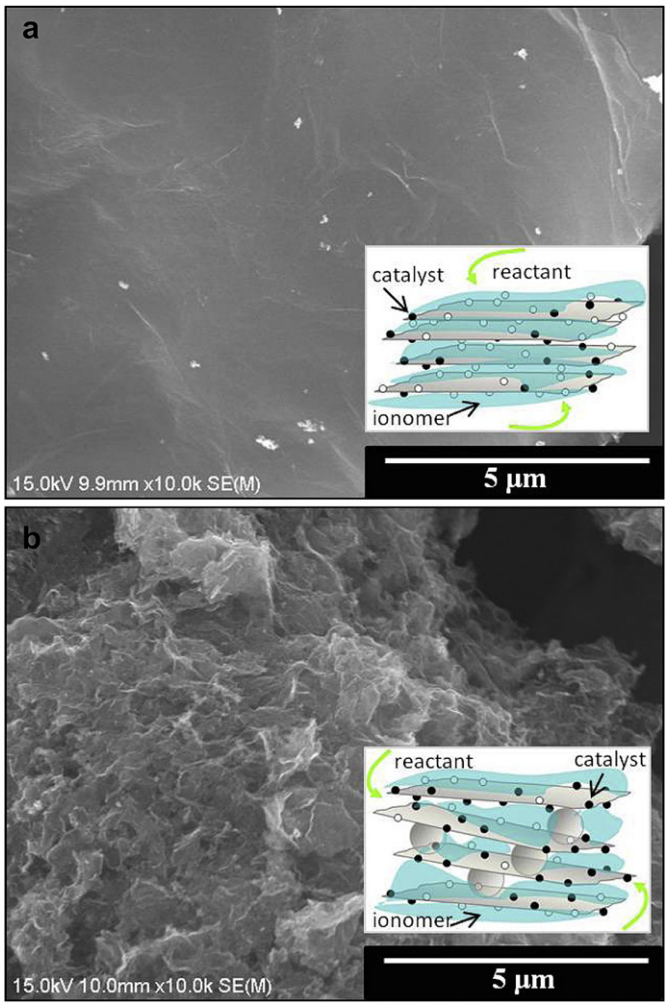

Fig. 4. FE-SEM images of (a) PtRu/graphene and (b) PtRu/graphene–Vulcan carbon composite. The inserts show the effects of a spacing material between two-dimensional graphene (●: activated catalyst, ○: dead catalyst).

Tech, Inc. 890 series, GT-500). The cell temperature was maintained at 70 °C with the H_2 and air gases humidified at 80 °C for anode and 75 °C for cathode, respectively.

3. Results and discussion

Surface chemical information was obtained using X-ray photoelectron spectroscopy (XPS). The main signals present on the survey spectra of the graphene oxide and graphene are due to C and O. The high-resolution C 1s XPS spectra are shown in Fig. 2(a). The C 1s peak of the graphene oxide consists of C–C (sp^2 carbon in the basal plan, 284.6 eV), C–O (286.6 eV), C=O (288.1 eV) and O–C=O (289 eV). The contribution of C–O is particularly high. After a reduction using formaldehyde, the O/C ratio decreases notably in graphene, indicating that a large majority of the oxygenated species is removed [24,25]. In addition, a broad and weak peak centered above 290.0 eV is identified as a shake-up satellite due to $\pi-\pi^*$ transitions [26]. To assess the reduction of graphene oxide, Fourier transform infrared (FT-IR) spectra of the nanostructures were recorded (Fig. 2(b)). The FT-IR spectrum of graphene oxide shows the presence of various oxygen-containing groups, including O–C=O ($\nu_{O-C=O}$ at 840 cm^{-1}), C–OH (ν_{C-OH} at 1220 cm^{-1}), O–H (ν_{O-H} at 1400 cm^{-1}) and carboxyl functional moieties at 1730 cm^{-1}, which are formed owing to the strong oxidation process [27]. On the other hand, in the case of graphene, most of the contributions from the oxygen-containing groups decrease after reduction using formaldehyde. Tapping-mode atomic force microscopy (AFM) shows that the graphene sheet was flat, with a thickness of ~1.48 nm (Fig. 2(c)). The measured thickness is larger than the theoretical value of a perfectly flat sp^2-carbon atom network (~0.32 nm). It is assumed that this difference results from oxygen-containing functionalities such as epoxy and hydroxyl groups, intrinsic out-of-plane deformation of graphene, and an instrumental offset arising from different interactions between the AFM cantilever, graphene sheet, and substrate [21,24]. The crystal structures of the graphene oxide, graphene sheet and prepared

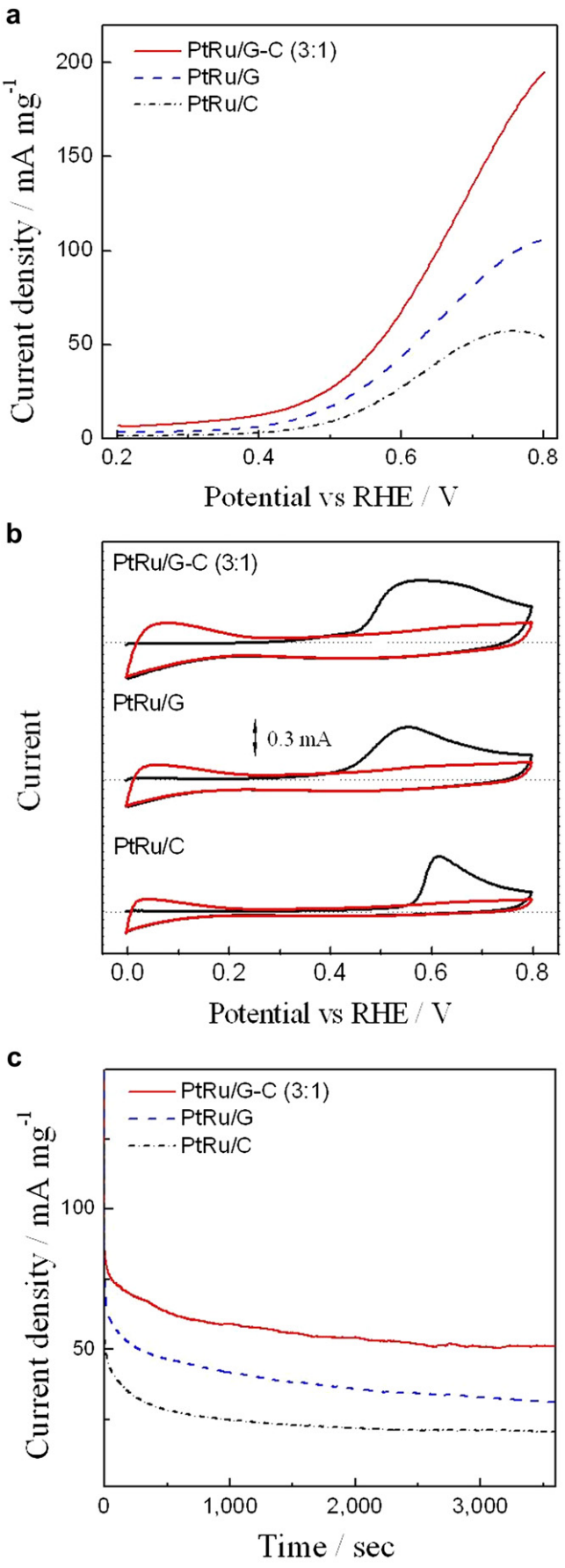

catalysts were characterized using XRD, the results of which are shown in Fig. 3(a). The XRD pattern of graphene oxide showed a well-defined (002) peak at 10.5°. After a chemical reduction using formaldehyde, the graphene oxide was reduced to graphene with a peak at 24.7° [22]. Additionally, XRD data of PtRu catalysts loaded onto supporting materials are shown in Fig. 3(a). The Pt (111) peak observed from all alloy catalysts shifts slightly toward a higher value compared with pure Pt. This shift indicates that the alloy is formed between the Pt and Ru [22,28].

The surface morphology of the PtRu/graphene–Vulcan carbon was observed using a high-resolution transmission electron microscopy (HR-TEM) and field-emission scanning electron microscopy (FE-SEM). As shown in Fig. 3(b), PtRu nanoparticles were uniformly dispersed on a graphene–Vulcan carbon composite and their ranges were primarily between 1 and 5 nm with an average particle size of 3.3 nm, which is slightly smaller than PtRu/Vulcan carbon with an average particle size of about 3.5 nm (Fig. S1 in the Supplementary information). The graphene consists of randomly aggregated, closely associated crumpled sheets forming a disordered solid. The PtRu/graphene catalyst (Fig. 4(a)) shows a slightly wrinkled morphology, while the PtRu/graphene–Vulcan carbon composite shows a highly wrinkled morphology (Fig. 4(b)). Aksay et al. reported that these wrinkles may be important for preventing the aggregation of graphene occurring from van der Waals forces during drying process and to maintain high active surface area [7,18]. This means that the Vulcan carbon prevents the aggregation of graphene sheets and increases distance between them, thereby altering their arrays. An effective electrocatalyst is one that correctly balances the transport processes required for an operational fuel cell. A catalyst, ionomer and reactant are referred to as a triple-phase found in a catalyst layer. The triple-phases meet at the triple-phase boundary and create a reaction carried out by the catalyst particles [29]. In the PtRu/graphene, a relatively low triple-phase boundary resulted from the aggregation of the graphene sheets. In contrast, more triple-phase boundaries could be created in a PtRu/graphene–Vulcan carbon than in a PtRu/graphene owing to the well-arranged spacing structure of a graphene–Vulcan carbon composite. Therefore, the catalyst layer with a graphene–Vulcan carbon composite provides more reactive PtRu nanoparticles adjacent with an ionomer and reactant, resulting in a higher methanol oxidation and ESA (Fig. 5). The electrocatalytic activity for methanol oxidation was estimated by linear sweep voltammetry. Fig. 5(a) shows the linear sweep voltammograms of the PtRu/graphene–Vulcan carbon composite (PtRu/G–C), PtRu/graphene (PtRu/G), and PtRu/Vulcan carbon (PtRu/C) in 1 M CH_3OH and 1 M H_2SO_4. The current density of the PtRu/G–C catalyst was increased to twice that of the PtRu/G catalyst at 0.8 V. The electrocatalysts with different graphene–Vulcan carbon ratio were prepared and their electrochemical activities evaluated (Fig. S1 in the Supplementary information). PtRu/graphene–Vulcan carbon at 3:1 w/w shows the highest methanol oxidation compared to the other composition ratios. This ratio suggests the best electrocatalyst activity during methanol oxidation.

The electrochemically active surface area (ESA) provides important information regarding the number of available active

Fig. 5. (a) Linear sweep voltammograms of the prepared catalysts in 1 M H_2SO_4 and 1 M CH_3OH at 25 °C at a scan rate of 20 mV s^{-1}. (b) CO-stripping voltammograms in 1 M H_2SO_4. The black line shows the first cycle, i.e., the CO-stripping voltammograms, while the red line shows the second cycles, which are equivalent to the background CV of the particular catalysts. (c) Chronoamperometric curves at 0.7 V in 1 M CH_3OH and 1 M H_2SO_4. (For interpretation of the references to color in this figure legend, the reader is referred to the web version of this article.)

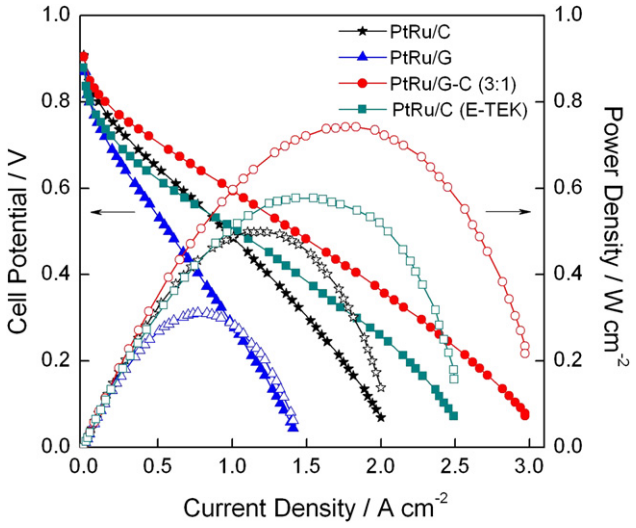

Fig. 6. (a) Current–voltage polarization curves of the polymer electrolyte membrane fuel cell using PtRu/Vulcan carbon, PtRu/graphene, PtRu/Vulcan carbon–graphene (3:1), and commercial catalysts (E-TEK, 40 wt.% PtRu/C) as respective anode electrocatalyst. The cell temperature was maintained at 70 °C with the anode (H_2) and cathode (air) gases humidified at 80 °C and 75 °C, respectively.

sites. Fig. 5(b) shows the CO-stripping voltammograms of the PtRu/graphene–Vulcan carbon (PtRu/G–C), PtRu/graphene (PtRu/G), and PtRu/Vulcan carbon (PtRu/C) recorded in 1 M H_2SO_4 at a scan rate of 20 mV s^{-1}. Note that the PtRu/G–C catalyst of 79.8 m^2 g^{-1} exhibits a larger electrochemical surface area than the PtRu/G catalyst value of 44.6 m^2 g^{-1}, which is attributed to the different active sites. Long-term methanol oxidation was conducted at 0.7 V and the variation of current with time was recorded (Fig. 5(c)). The performances of the prepared catalysts show that the current density initially decreased and reached a steady state value. From these results, the PtRu/G–C catalyst exhibits a higher current density and long-term performance for the methanol oxidation compared with PtRu/G and PtRu/C. Fig. 6 shows the polarization curves of the polymer electrolyte membrane fuel cell using the as-prepared catalysts and the commercial catalysts. The current densities at 0.6 V are 0.967 A cm^{-2} and 0.368 A cm^{-2} for the 40 wt.% PtRu/G–C (3:1 w/w) and 40 wt.% PtRu/graphene, respectively. The power densities of the PtRu/G–C (3:1 w/w) and PtRu/graphene were found to be 0.742 W cm^{-2} and 0.310 W cm^{-2}, respectively. It is evident from Fig. 6 that the PtRu/G–C (3:1 w/w) catalyst exhibited better performance than that of the PtRu/graphene catalyst in a polymer electrolyte membrane fuel cell test. The results indicated that Vulcan carbon effectively modifies to array of graphene sheets, resulting in more triple-phase boundaries available for electrochemical reaction and better mass transport in the catalyst layer.

4. Conclusions

In this research, we prepare a graphene through a simple chemical oxidation and loaded 40 wt.% PtRu onto a graphene–Vulcan carbon composite using an improved impregnation method. Vulcan carbon is added as a nano spacer to enhance the utilization and electrochemical activities of the graphene-based materials. The results show that a PtRu catalyst loaded onto the graphene–Vulcan carbon (3:1 w/w) composite exhibits high electrocatalytic activity and high stability toward methanol electrochemical oxidation owing to the special structure of the graphene–Vulcan carbon composite. Also, the PtRu/graphene–Vulcan carbon catalyst exhibits better performance than the PtRu/graphene catalyst in a polymer electrolyte membrane fuel cell test. These results indicate that a graphen–Vulcan carbon composite is a good candidate for a supporting material in fuel cells.

Acknowledgments

This work was supported by the Smart IT Convergence System Research Center funded by the Ministry of Education, Science and Technology as Global Frontier Project (0543-20110015). This work was also supported by Nano·Material Technology Development Program through the National Research Foundation of Korea (NRF) funded by the Ministry of Education, Science and Technology (2011-0030266) and the National Research Foundation of Korea grant funded by the Korea Government (MEST) (No. 2007-0056334).

Appendix A. Supporting information

Supplementary data related to this article can be found at http://dx.doi.org/10.1016/j.jpowsour.2012.07.115.

References

[1] K.I. Han, J.S. Lee, S.O. Park, S.W. Lee, Y.W. Park, H. Kim, Electrochim. Acta 50 (2000) 791.
[2] K. Park, Y. Sung, S. Han, Y. Yun, T. Hyeon, J. Phys. Chem. B 108 (2004) 939.
[3] E. Antolini, Appl. Catal. B 88 (2009) 1.
[4] K.S. Novoselov, A.K. Geim, S.V. Morozov, D. Jiang, Y. Zhang, S.V. Dubonos, I.V. Grigorieva, A.A. Firsov, Science 306 (2004) 666.
[5] A.K. Geim, K.S. Novoselov, Nat. Mater. 6 (2007) 183.
[6] B. Seger, P.V. Kamat, J. Phys. Chem. C 113 (2009) 7990.
[7] R. Kou, Y. Shao, D. Wang, M.H. Engelhard, J.H. Kwak, J. Wang, V.V. Viswanathan, C. Wang, Y. Lin, Y. Wang, I.A. Aksay, J. Liu, Electrochem. Commun. 11 (2009) 954.
[8] Y. Xin, J. Liu, Y. Zhou, W. Liu, J. Gao, Y. Xie, Y. Yin, Z. Zou, J. Power Sources 196 (2011) 1012.
[9] D.A.C. Brownson, D.K. Kampouris, C.E. Banks, J. Power Sources 196 (2011) 110.
[10] S. Bong, Y. Kim, I. Kim, S. Woo, S. Uhm, J. Lee, H. Kim, Electrochem. Commun. 12 (2010) 129.
[11] Q. Shi, S. Mu, J. Power Sources 203 (2012) 48.
[12] H. Huang, H. Chen, D. Sun, X. Wang, J. Power Sources 204 (2012) 46.
[13] M.S. Wietecha, J. Zhu, G. Gao, N. Wang, H. Feng, M.L. Gorring, M.L. Kasner, S. Hou, J. Power Sources 198 (2012) 30.
[14] S. Park, R.S. Ruoff, Nat. Nanotechnol. 4 (2009) 217.
[15] W. Yang, K.R. Ratinac, S.P. Ringer, P. Thordarson, J.J. Gooding, F. Braet, Angew. Chem. Int. Ed. 49 (2010) 2114.
[16] D. Li, M.B. Muller, S. Gilje, R.B. Kaner, G.G. Wallace, Nat. Nanotechnol. 3 (2008) 101.
[17] H.C. Schniepp, J. Li, M.J. McAllister, H. Sai, M. Herrera-Alonso, D.H. Adamson, R.K. Prud'homme, R. Car, D.A. Saville, I.A. Akasy, J. Phys. Chem. B 110 (2006) 8535.
[18] M.J. McAllister, J. Li, D.H. Adamson, H.C. Schniepp, A.A. Abdala, J. Liu, M. Herrera-Alonso, D.L. Milius, R. Car, R.K. Prud'homme, I.A. Aksay, Chem. Mater. 19 (2007) 4396.
[19] N.I. Kovtyukhova, P.J. Ollivier, B.R. Martin, T.E. Mallouk, S.A. Chizhik, E.V. Buzaneva, A.D. Gorchinskiy, Chem. Mater 11 (1999) 771.
[20] A.J. Patil, J.L. Vickery, T.B. Scott, S. Mann, Adv. Mater. 21 (2009) 3159.
[21] Y. Kim, S. Bong, Y. Kang, Y. Yang, R.K. Mahajan, J.S. Kim, H. Kim, Biosens. Bioelectron 25 (2010) 2366.
[22] I. Kim, S. Bong, S. Woo, R.K. Mahajan, H. Kim, Int. J. Hydrogen Energy 36 (2011) 1803.
[23] Y. Takasu, T. Fujiwara, Y. Murakami, K. Sasaki, M. Oguri, T. Asaki, W. Sugimoto, J. Electrochem. Soc. 147 (2000) 4421.
[24] X. Fan, W. Peng, Y. Li, X. Li, S. Wang, G. Zhang, F. Zhang, Adv. Mater. 20 (2008) 4490.
[25] J. Yan, T. Wei, B. Shao, F. Ma, Z. Fan, M. Zhang, C. Zheng, Y. Shang, W. Qian, F. Wei, Carbon 48 (2010) 1731.
[26] S. Park, S. Yu, N. Pinna, S. Woo, B. Jang, Y. Chung, Y. Cho, Y. Sung, Y. Piao, J. Mater. Chem. 22 (2012) 2520.
[27] R. Bissessur, P.K.Y. Liu, W. White, S.F. Scully, Langmuir 22 (2006) 1729.
[28] J. Guo, G. Sun, Q. Wang, G. Wang, Z. Zhou, S. Tang, L. Jiang, B. Zhou, Q. Xin, Carbon 44 (2006) 152.
[29] S. Litster, G. McLean, J. Power Sources 130 (2004) 61.